PHYSICAL REVIEW A **91**, 013623 (2015)

Signature of the existence of a coherently condensed state in a dilute gas above the Bose-Einstein-condensate transition temperature

Yinbiao Yang and Wen-ge Wang*

Department of Modern Physics, University of Science and Technology of China, Hefei 230026, China

(Received 18 August 2014; published 21 January 2015)

We study quantum coherence properties of a dilute gas at temperatures above, but not much above, the transition temperature of Bose-Einstein condensation. In such a gas, a small proportion of the atoms may possess coherence lengths longer than the mean neighboring-atomic distance, implying the existence of quantum coherence greater than that expected for thermal atoms. Conjecturing that a part of this proportion of the atoms may lie in a coherently condensed state, some unexplained experimental results [D. E. Miller *et al.*, Phys. Rev. A **71**, 043615 (2005)] can be explained.

DOI: 10.1103/PhysRevA.91.013623 PACS number(s): 03.75.Nt, 03.75.Hh, 67.85.−d, 03.65.Yz

I. INTRODUCTION

Quantum coherence at the macroscopic and mesoscopic scales is a topic of interest in a variety of fields. A well-known example is the Bose-Einstein condensation (BEC) formed in a dilute gas of identical atoms when the temperature is dropped below the transition temperature T_c [1–7]. One interesting question is whether, at temperatures above and within the same order of magnitude as T_c, atoms may possess quantum coherence greater than that expected for thermal atoms. In fact, at temperatures a little above T_c, the stochastic Gross-Pitaevskii equation approach predicts that a fraction of the atoms may still lie in a BEC-type state [8]. Some other approaches give more or less similar predictions, restricted to the region around T_c [9–17]. However, for temperatures several times higher than T_c, these theoretical approaches do not give a clear prediction for the above-mentioned quantum coherence.

Interestingly, on the other hand, experimental evidence exists for the above-discussed quantum coherence. It is given by a recent experiment in which contrasts of the interference patterns formed by a dilute gas of atoms were measured [18]. It was observed that, at some temperatures above T_c and under some values of controlling parameters, the measured contrasts are obviously higher than those predicted for thermal atoms, implying the existence of extra quantum coherence. A theoretical explanation for this extra coherence is still absent, and the purpose of this paper is to take a first step toward it.

To explain the approach we are to take, let us first consider a gas of thermal (identical) atoms at a temperature much higher than T_c. At such a high temperature, the indistinguishability of the atoms usually does not have a significant effect, and as a result, the atoms can be treated effectively as distinguishable particles. As an approximation, a single atom in the gas can be treated as a quantum Brownian particle interacting with a thermal bath. Below, we call this approximation the *distinguishable-particle approximation*. Behaviors of a quantum Brownian particle have been studied extensively in past years (see, e.g., Refs. [19–25] and references therein). Due to environment-induced decoherence [26–30], the reduced state of the particle may approach an approximately diagonal form in a basis given by Gaussian wave packets [22,23], which is usually referred to as the preferred (pointer) basis [28–31]. This implies that the atom can be effectively described by a mixture of Gaussian packets.

The width of the Gaussian wave packet discussed above gives a measure of the coherence length of the related atom. It cannot remain constant due to wave-packet expansion [33]. An intriguing question is what may happen to those atoms whose coherence lengths are on the scale of the mean neighboring-atomic distance. The above-discussed distinguishable-particle approximation fails for these atoms, since the related Gaussian packets usually have non-negligible overlap with those of the neighboring atoms. It would be reasonable to expect that these atoms, at least some of them, may possess coherence greater than that expected for thermal atoms.

At high temperatures, the proportion of the above-discussed atoms with long coherence lengths should be too small to induce any notable effect in most cases. However, when the temperature drops to the order of T_c, attention should be paid to them. In fact, as is well known, when the temperature becomes close to T_c, the thermal de Broglie wavelength reaches the scale of the mean neighboring-atomic distance [5]. In addition, the mean coherence length of the atoms, given by the mean width of the related Gaussian wave packets, is of the order of the thermal de Broglie wavelength [23]. These two points suggest an intuitive picture of a gas entering a BEC state, that is, loosely speaking, it may happen when the mean coherence length obtained under the distinguishable-particle approximation reaches the scale of the mean neighboring-atomic distance. Based on this picture, it would be reasonable to assume that (some of) the atoms with sufficiently long coherence lengths may form a condensate with strong coherence, such that they may generate an interference pattern like that of a BEC. We call such a condensate state a *coherently condensed state*.

In this paper, we show that, making use of the above-discussed assumption about the existence of a coherently condensed state of some atoms, we can arrive at a semiquantitative explanation for the main features of the experimentally observed, unexpectedly high contrasts discussed above. Specifically, the paper is organized as follows. In Sec. II, we discuss two models for a gas at temperatures above T_c: a simple thermal model, in which the atoms are treated as

*wgwang@ustc.edu.cn

thermal atoms, and a hybrid model, in which most the atoms are thermal atoms while a small proportion of the atoms lies in a coherently condensed state. Based on decoherence arguments, we derive an expression for the temperature dependence of the proportion of the atoms with long coherence lengths. In Sec. III, we discuss predictions of the hybrid model for the contrasts of the interference patterns studied in the experiments in Ref. [18] and compare the predictions with experimental results. Finally, concluding remarks and discussions are given in Sec. IV.

II. TWO MODELS FOR A GAS OF ATOMS AT TEMPERATURES ABOVE T_c

In this section, we discuss two models for a gas of N identical, bosonic atoms: a simple thermal model for high temperatures in Sec. II A and a hybrid model for temperatures above and of the order of the BEC-transition temperature T_c in Sec. II B. In Sec. II C, we discuss the temperature dependence of the proportion of atoms possessing long coherence lengths.

A. A simple thermal model for high temperatures

We neglect the internal motion of the atoms. At high temperatures with $T \gg T_c$, as discussed in Sec. I, one may use the distinguishable-particle approximation. At the end of this section, we report that this approximation leads to a self-consistent picture for the motion of most of the atoms.

We use S to denote a considered, central atom, and $\mathcal{E}$ to denote the rest of the atoms, as the environment of S. The state of the total system is denoted $|\Psi\rangle$. Assuming that the environment can be regarded as a heat bath, the central atom behaves like a particle undergoing a quantum Brownian motion, which has been extensively studied [19–25]. It is known that, for such a particle, the minimal-uncertainty Gaussian states are approximately preferred states, and in the basis of these states, the reduced density matrix, $\rho^{\rm re} = {\rm Tr}_{\mathcal{E}}(|\Psi\rangle\langle\Psi|)$, approaches an approximate diagonal form beyond some finite time scale [23],

$$\rho^{\rm re}(t) \approx \int {\rm d}\mu_\alpha \rho_\alpha(t)|\alpha\xi_0\rangle\langle\alpha\xi_0|. \tag{1}$$

Here, $|\alpha\xi\rangle$ indicates a minimal-uncertainty Gaussian state, centered at $\alpha = (\mathbf{x}_0,\mathbf{p}_0)$ in the phase space and possessing a dispersion ξ in the coordinate space, whose wave function in the coordinate space is a Gaussian wave packet of the form

$$\varphi(\mathbf{x};\alpha,\xi) = A_\xi^3 \exp\left[\frac{i\boldsymbol{p}_0\cdot(\boldsymbol{x}-\boldsymbol{x}_0)}{\hbar} - \frac{(\boldsymbol{x}-\boldsymbol{x}_0)^2}{4\xi^2}\right], \tag{2}$$

where $\hbar$ is the Planck constant and

$$A_\xi = (2\pi)^{-1/4}\xi^{-1/2} \tag{3}$$

is the normalization coefficient. As is well known, this Gaussian state is a coherent state [32].

The reduced density matrix in Eq. (1) suggests that, effectively, the central atom may be described by a mixture of Gaussian wave packets, with probabilities ρ_α. If, further assuming that $\rho_\alpha(t)$ has reached a stationary solution with a Boltzmann form, then one gets a simple thermal model for the atoms in an equilibrium state, which was used in Ref. [18].

The dispersion ξ_0 in Eq. (1) is fixed and temperature dependent [23],

$$\xi_0 = \frac{\hbar}{\sqrt{2mk_BT}} = \frac{1}{2\sqrt{\pi}}\lambda_T, \tag{4}$$

where λ_T is the thermal de Broglie wavelength and k_B denotes the Boltzmann constant. As pointed in Ref. [33], due to wave-packet expansion, the dispersion of the packet in fact cannot remain constant. The above-discussed fixed value of ξ_0 can be regarded as the mean value of the dispersion. At $T \gg T_c$, ξ_0 is much smaller than the mean distance between neighboring atoms, denoted d_a in what follows. As a result, most of the Gaussian packets of neighboring atoms have negligible overlap in the coordinate space. This justifies the validity of the distinguishable-particle approximation.

B. A hybrid model for T of the order of T_c

When the temperature T drops to the order of T_c, the dispersion of the packets discussed above reaches the order of d_a on average, hence, its variation can no longer be neglected. To study the properties of the central atom in this case, we expand the state vector of the total system in the following form, with the dispersion ξ as a variable,

$$|\Psi(t)\rangle = \int d\mu_\alpha d\xi|\alpha\xi\rangle\big|\Phi_{\alpha\xi}^{\mathcal{E}}(t)\big\rangle, \tag{5}$$

where $|\Phi_{\alpha\xi}^{\mathcal{E}}(t)\rangle$ are the corresponding components of the environment. We assume that decoherence has occurred, such that the Gaussian states are approximately preferred states [33] and the components $|\Phi_{\alpha\xi}^{\mathcal{E}}(t)\rangle$ of the environment satisfy

$$\big\langle\Phi_{\alpha'\xi'}^{\mathcal{E}}(t)\big|\Phi_{\alpha\xi}^{\mathcal{E}}(t)\big\rangle \approx 0 \tag{6}$$

for α not close to α' and for ξ not close to ξ'. Then the reduced density matrix has approximately the "diagonal" form

$$\rho^{re}(t) \approx \int d\mu_\alpha d\xi \rho_{\alpha\xi}(t)|\alpha\xi\rangle\langle\alpha\xi|, \tag{7}$$

where

$$\rho_{\alpha\xi}(t) = \big\langle\Phi_{\alpha\xi}^{\mathcal{E}}(t)\big|\Phi_{\alpha\xi}^{\mathcal{E}}(t)\big\rangle. \tag{8}$$

According to Eq. (7), effectively, the atom can be regarded as lying in a mixed state, i.e., in a mixture of $|\alpha\xi\rangle$ with probabilities $\rho_{\alpha\xi}(t)$.

In the mixed-state description discussed above, the Gaussian wave packets of $|\alpha\xi\rangle$ with large dispersions, $\xi \gtrsim d_a$, may induce a problem. That is, they usually have non-negligible overlap with Gaussian wave packets of their neighboring atoms, and as a result, symmetrization of the whole wave function does not allow us to treat the atoms as distinguishable particles. This is in conflict with the distinguishable-particle approximation, which is the starting point of the above approach. This confliction suggests that the related atoms may possess quantum coherence greater than that expected for uncorrelated thermal atoms.

Then, what type of quantum coherence might the corresponding atoms have? As discussed in Sec. I, for temperatures a little above T_c, some fraction of the atoms may lie in a BEC state. It would be natural to expect that, at temperatures not very close to T_c but still of the order of T_c, a small proportion of the atoms may lie in a state with some similarity to a BEC state. In particular, we recall that, as discussed previously, loosely speaking, BEC transition happens when the mean coherence length of the atoms obtained in the distinguishable-particle approximation, which is of the order of the thermal de Broglie wavelength, reaches the order of the mean neighboring-atomic distance d_a.

Based on the above understanding of BEC transition, we make the following conjecture, which is the basic assumption of this paper:

> Atoms that are connected by the relation of mutual coherence, defined below, may lie in a coherently condensed state and can be described by the same single-particle state.

Here, two atoms are said to have a *mutual-coherence* relation if they are associated with two Gaussian wave packets whose coherence lengths are longer than the distance between the centers of the two packets. Two atoms in mutual coherence with the same third atom are regarded as being in mutual coherence too. Clearly, the atoms connected by the relation of mutual coherence can be regarded as a whole.

At temperatures T above and not far from T_c, most of the atoms with $\xi \gtrsim d_a$ are connected by the mutual-coherence relationship. The above-discussed conjecture implies that these atoms lie in a coherently condensed state. Then, using $P_{\rm con}$ to denote the probability that an atom will lie in a coherently condensed state, we have

$$P_{\rm con}(t) = \int_{d_c}^{\infty} P(\xi,t) d\xi, \tag{9}$$

where d_c is of the order of d_a and $P(\xi,t)$ indicates the probability that an atom will have a coherence length characterized by ξ [34], namely,

$$P(\xi,t) = \int d\mu_\alpha \rho_{\alpha\xi}(t). \tag{10}$$

In what follows, for simplicity of discussion, we assume that $d_c = d_a$, since generalization of the results given below to the case of d_c not equal to d_a is straightforward.

Finally, we get the following hybrid model for a gas in an equilibrium state with a temperature T above and of the order of T_c. That is, the atoms associated with $|\alpha\xi\rangle$ of $\xi \gtrsim d_a$ lie in a coherently condensed state, while other atoms are thermal atoms described by the simple thermal model discussed in the previous section. According to the conjecture introduced above, atoms lying in the coherently condensed state can be described by the same single-particle wave function when computing the interference pattern they generate.

C. Temperature dependence of $P_{\rm con}$

In this section, we discuss the dependence of $P_{\rm con}$ on the temperature T. Let us first discuss the time variation of $P(\xi,t)$ in Eq. (10). It is mainly determined by competition of the following two aspects of the Schrödinger evolution of $|\alpha\xi\rangle|\Phi^{\mathcal{E}}_{\alpha\xi}(t)\rangle$ on the right-hand side of Eq. (5). On one hand, expansion of the wave packet $|\alpha\xi\rangle$ converts $\rho_{\alpha\xi}$ in Eq. (8) to $\rho_{\alpha'\xi'}$ with a larger dispersion $\xi' > \xi$. On the other hand, the interaction between the central atom and other atoms may induce decoherence, changing $|\alpha\xi\rangle|\Phi^{\mathcal{E}}_{\alpha\xi}\rangle$ to a superposition of $|\alpha'\xi'\rangle|\Phi^{\mathcal{E}}_{\alpha'\xi'}\rangle$ with smaller dispersions $\xi' < \xi$ and with almost-orthogonal $|\Phi^{\mathcal{E}}_{\alpha'\xi'}\rangle$. This decoherence process converts $\rho_{\alpha\xi}$ to $\rho_{\alpha'\xi'}$ with a smaller dispersion $\xi' < \xi$. Therefore, the probability $P(\xi,t)$ at a time t has two sources: The first is due to wave-packet expansion from $|\alpha'\xi'\rangle|\Phi^{\mathcal{E}}_{\alpha'\xi'}(t')\rangle$ with $\xi' < \xi$ at some previous time t', and the second is due to decoherence from $|\alpha''\xi''\rangle|\Phi^{\mathcal{E}}_{\alpha''\xi''}(t'')\rangle$ with $\xi'' > \xi$ at some previous time t''.

In Eq. (9), only those $P(\xi,t)$ with $\xi \geqslant d_a$ contribute to $P_{\rm con}$. At temperatures T obviously higher than (still of the order of) T_c, d_a is obviously larger than the mean value of ξ. Physically, one can assume that $P(\xi,t)$ decreases sufficiently rapidly with increasing ξ beyond $\xi = d_a$. (Later we show that this assumption leads to a self-consistent result.) Hence, for $P(\xi,t)$ with $\xi \geqslant d_a$, the above-discussed contribution from the second source is small, compared with that from the first one, and can be neglected.

Then, for large ξ, we get the expression for $P(\xi,t)$, in terms of $P(\xi',t')$ with $\xi' < \xi$ and $t' < t$,

$$P(\xi,t) \approx P(\xi',t') - \eta_{\tau}(\xi')P(\xi',t')\Delta t, \tag{11}$$

where $\Delta t = t - t'$, the second term on the right-hand side represents the effect of decoherence which converts $|\alpha'\xi'\rangle|\Phi^{\mathcal{E}}_{\alpha'\xi'}\rangle$ to superpositions of narrower wave packets of the central atom, and $\eta_{\tau}(\xi')$ indicates the rate of this decoherence process. The two variables ξ and ξ' are connected by the relation $\xi = \xi' + v_e\Delta t$, where v_e is the expanding speed of the packet. The speed v_e is determined by the width of the initial packet, whose expansion makes contributions to both $P(\xi,t)$ and $P(\xi',t')$, hence, v_e is ξ independent. Since as discussed above the dispersion ξ has a mean value given by ξ_0 in Eq. (4), in most cases v_e is approximately determined by ξ_0, hence, it is temperature dependent. According to standard textbooks [see Eq. (29)], $v_e \propto 1/\xi_0$, and as a result, $v_e \propto T^{1/2}$. Therefore, we write $v_e = u_0T^{1/2}$ with u_0 approximately temperature independent.

In an equilibrium state, the probability $P(\xi,t)$ is time independent, denoted $P(\xi)$. For large ξ, Eq. (11) shows that this distribution satisfies

$$\frac{\mathrm{d}P(\xi)}{\mathrm{d}\xi} \approx -\frac{\eta_{\tau}(\xi)}{u_0T^{1/2}}P(\xi), \tag{12}$$

where $v_e = u_0T^{1/2}$ has been used. Equation (12) has a solution,

$$P(\xi) \approx a_0 \exp\left\{-\frac{1}{u_0T^{1/2}}\int \mathrm{d}\xi\,\eta_{\tau}(\xi)\right\}, \tag{13}$$

where a_0 is an integration constant.

We assume that the decoherence rate $\eta_{\tau}(\xi)$ has the following dependence on ξ and T,

$$\eta_{\tau}(\xi) \simeq a_1\xi^{\gamma}T^{\beta}, \tag{14}$$

with a parameter a_1 independent of ξ and T. To get the values of γ and β, we note that the decoherence is induced by collisions among the atoms. This implies that, approximately, η_{τ} should be proportional to the number of collisions per time unit. First, it should be proportional to the mean speed of the atoms, hence, $\eta_{\tau} \sim \sqrt{T}$, giving $\beta = 1/2$. Second, since the collision number is approximately proportional to the cross sections of the Gaussian packets, one has $\eta_T \sim \xi^2$, giving $\gamma = 2$. For $\beta = 1/2$ and $\gamma = 2$, Eq. (13) gives

$$P(\xi) \approx a_0 \exp\left\{-\frac{a_1}{3u_0}\xi^3\right\}. \tag{15}$$

Equation (15) shows that our previous assumption about the fast decay of $P(\xi,t)$ for large ξ is self-consistent.

As for the parameter a_0, we note that due to the T dependence of the decoherence rate $\eta_T(\xi)$ with $\beta = 1/2$, the variation rate of $P(\xi)$ in Eq. (12) with respect to ξ is in fact T independent. This suggests that the parameter a_0 may be T independent. Below, we assume that a_0 either is T independent or changes slowly with T.

Now we compute the proportion $P_{\rm con}$. Substituting Eq. (13) with Eq. (14) into Eq. (9), direct derivation shows that, in terms of $z = (\xi/d_a)^{\gamma+1}$, $P_{\rm con}$ can be written as

$$P_{\rm con} \approx \frac{d_a a_0}{\gamma+1}\int_1^\infty {\rm d}z z^{-\frac{\gamma}{\gamma+1}} \exp\left(-\frac{a_1 d_a^{\gamma+1}}{(\gamma+1)u_0}T^{\beta-1/2}z\right). \tag{16}$$

In the experiment we discuss, the mean atomic distance d_a is proportional to $\sqrt{T}$, therefore, we write

$$d_a = a_2 T^{1/2} \tag{17}$$

[see Eq.(25) for an explicit expression of d_a]. Then, noting that u_0, a_1, and a_2 are ξ independent, we have

$$P_{\rm con} \approx a_c T^{1/2} E_{\frac{\gamma}{\gamma+1}}\left(\left(\frac{T}{T_0}\right)^{\gamma/2+\beta}\right), \tag{18}$$

where $E_n(x)$ is a function defined by

$$E_n(x) = \int_1^\infty z^{-n}e^{-xz}dz, \tag{19}$$

and

$$T_0 = \left[\frac{a_1 a_2^{\gamma+1}}{(\gamma+1)u_0}\right]^{-\frac{1}{\gamma/2+\beta}}, \tag{20}$$

$$a_c = \frac{a_0 a_2}{\gamma+1}. \tag{21}$$

The proportion $P_{\rm con}$ has an exponential-type decay in the temperature region of interest here (see Fig. 1).

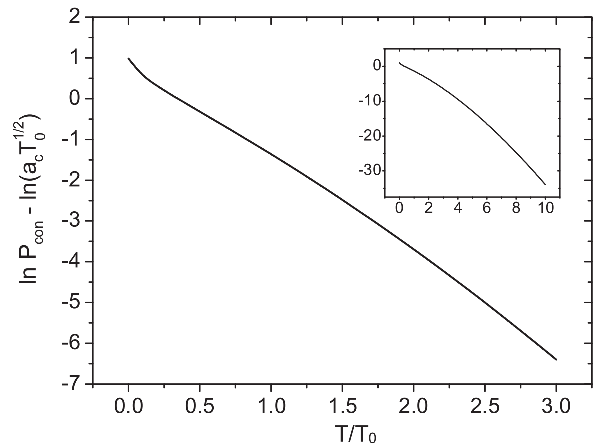

FIG. 1. Variation of $P_{\rm con}/(a_c T_0^{1/2})$, on the logarithmic scale, with T/T_0 for $\gamma = 2$ and $\beta = 0.5$ [see Eq. (18)]. It shows an approximately exponential decay for T below $3T_0$. Inset: The decay is even faster for larger T/T_0.

III. EXPERIMENTAL EVIDENCE OF THE EXISTENCE OF A COHERENTLY CONDENSED STATE ABOVE T_c

In this section, we show that some of the unexplained experimental results given in Ref. [18] can be explained in the hybrid model introduced above.

A. Experimental results in Ref. [18]

In this subsection, we summarize experimental results given in Ref. [18], which are of relevance to the study in this paper. In an experiment discussed there, the contrast of the interference pattern formed by a cloud of N atoms with mass m is measured. Initially, the cloud, confined by a harmonic trap with a frequency ω, is prepared in a thermal state at a temperature T, which is above the BEC transition temperature T_c. Shortly after being released from the trap, the gas is exposed to two Bragg beams successively. Each Bragg beam has a shining period τ_p. This process creates an identical copy of the initial cloud, separated by a distance denoted d. Then the cloud and its copy expand freely and, after a period of flying time $\tau_f = 48$ ms, form an interference pattern with a contrast denoted $C_{\rm ex}$.

To analyze the experimental results, the simple thermal model discussed in Sec. II A was studied in Ref. [18], with the dispersion of the Gaussian packets given by the thermal de Broglie wavelength, $\lambda_T = h/\sqrt{2\pi m k_B T}$. This model predicts the contrast for the interference pattern

$$C_{\rm th} = \exp\left(-\frac{2\pi^2 R_T^2}{\lambda_f^2}\right), \tag{22}$$

where the subscript "th" stands for thermal, and

$$\lambda_f = \frac{h\tau_f}{md}, \quad R_T = \sqrt{\frac{k_B T}{m\omega^2}}. \tag{23}$$

The quantity λ_f gives the fringe spacing of the interference pattern.

The following results were reported in Ref. [18], concerning the contrast $C_{\rm ex}$.

(i) There exists approximately a temperature, which we denote T_d, below which $C_{\rm ex}$ values are close to $C_{\rm th}$ and above which $C_{\rm ex}$ values are higher than $C_{\rm th}$.

(ii) The temperature T_d changes notably with the shining length τ_p of the Bragg beams but is not as sensitive to the distance d.

(iii) The Bragg beams are velocity selective for a relatively long period τ_p.

More specifically, for point (ii), with $T_c \approx 0.6$ μK, in the case of $\tau_p = 10$ μs, $T_d \approx 3$ μK for $\lambda_f = 340$ μm, and $T_d \approx 2$ μK for both $\lambda_f = 230$ μm and $\lambda_f = 170$ μm. In the case of $\tau_p = 30$ μs, $T_d \approx 1$ μK for $\lambda_f = 170$ μm. Related to point (iii), within the simple thermal model, the velocity-selection effect cannot explain the observed, unexpectedly high contrast of C_{ex} at $T > T_d$ [18].

B. Detailed predictions of the simple thermal model

Before discussing predictions of the hybrid model and comparing them with the above-discussed experimental results, it would be useful to discuss in more detail predictions of the simple thermal model. In this model, when the cloud is released from the trap at an initial time $t = 0$, the atoms are described by an ensemble mixture of Gaussian wave packets $\varphi(\mathbf{x};\alpha,\xi)$ in Eq. (2). Let us consider a constant dispersion ξ of the order of the thermal de Broglie wavelength, $\xi \sim \lambda_T$. The values of α are assumed to obey the Boltzmann distribution,

$$f(\boldsymbol{x}_0,\boldsymbol{p}_0) = \left(\frac{\hbar\omega}{k_B T}\right)^3 \exp\left[-\frac{1}{k_B T}\left(\frac{\boldsymbol{p}_0^2}{2m} + \frac{m\omega^2 \boldsymbol{x}_0^2}{2}\right)\right], \tag{24}$$

where $m\omega^2 \boldsymbol{x}_0^2/2$ is the potential generated by the harmonic trap, centered at the origin of the coordinate space. Direct computation shows that, under this distribution, the standard deviation of the position of an atom in each direction is given by R_T in Eq. (23). Thus, the majority of the atoms lies within a sphere with a radius R_T. Using this property, we get the following estimate to the mean neighboring-atomic distance in the initial cloud:

$$d_a \approx R_T \left(\frac{4\pi}{3N}\right)^{1/3}. \tag{25}$$

Hence, the parameter a_2 in Eq. (17) has approximately the expression $a_2 \approx \sqrt{k_B/m\omega^2}\sqrt[3]{4\pi/3N}$.

Let us use t_b to denote a time immediately beyond the second Bragg beam. We assume that t_b is short, such that the wave packets still have a Gaussian shape. If a Bragg beam converts a packet into two packets, the two Bragg beams convert an initial Gaussian wave packet into four packets. Two in the four packets have the same mean velocity and we study the interference pattern formed by them. We use $\boldsymbol{d}$ to indicate the displacement of the two packets at this time, with $|\boldsymbol{d}| = d$, and take its direction as the x direction of the coordinate system. The z direction is taken to be perpendicular to the plane of the measured interference pattern.

The above-discussed two packets are written as

$$\psi(\boldsymbol{x},\alpha_0,t_b) = J[\psi_1(t_b) + \psi_2(t_b)], \tag{26}$$

where

$$\psi_1(t_b)\rangle \simeq \varphi(\boldsymbol{x};\alpha_1,\xi), \quad \psi_2(t_b) \simeq \varphi(\boldsymbol{x};\alpha_2,\xi), \tag{27}$$

with $\alpha_1 = (\boldsymbol{x}_0 + \frac{\boldsymbol{d}}{2},\boldsymbol{p}_0)$ and $\alpha_2 = (\boldsymbol{x}_0 - \frac{\boldsymbol{d}}{2},\boldsymbol{p}_0)$. For brevity, we normalize the wave function $\psi(\boldsymbol{x},\alpha,t_b)$, with

$$J = \left\{2 + 2\exp\left(-\frac{d^2}{8\xi^2}\right)\cos(\boldsymbol{p}_0\cdot\boldsymbol{d}/\hbar)\right\}^{-1/2}. \tag{28}$$

For the parameters used in the experiments and for $\xi \sim \lambda_T$, one has $\exp(-\frac{d^2}{8\xi^2}) \ll 1$. This gives $J \simeq 1/\sqrt{2}$.

To compute the Schrödinger evolution of $\psi_1(t)$ and of $\psi_2(t)$, we make use of a result given in standard textbooks, namely, an initial Gaussian wave packet $\varphi(\boldsymbol{x};\alpha_0,\xi)$ has the following free expansion [35],

$$A_\sigma^3 e^{i[\boldsymbol{p}_0\cdot(\boldsymbol{x}-\boldsymbol{x}_0)\hbar]} \times \exp\left\{\frac{-\left|\boldsymbol{x} - \left(\boldsymbol{x}_0 + \frac{\boldsymbol{p}_0 t}{m}\right)\right|^2}{4\sigma^2}\left(1 - \frac{i\hbar t}{2m\xi^2}\right) - i\theta(t)\right\}, \tag{29}$$

where A_σ is defined by Eq. (3) (with ξ replaced by σ),

$$\sigma = \sqrt{\left(\frac{\hbar t}{2m\xi}\right)^2 + \xi^2}, \tag{30}$$

and $\theta(t) = -\frac{\boldsymbol{p}_0^2 t}{2m\hbar} - \frac{3}{2}\arctan(\hbar t/2m\xi^2)$. Then it is not difficult to compute

$$\psi(\boldsymbol{x},\alpha_0,t) \simeq \frac{1}{\sqrt{2}}[\psi_1(t) + \psi_2(t)] \tag{31}$$

and the density $\rho(\boldsymbol{x},\alpha_0,t) = |\psi(\boldsymbol{x},\alpha_0,t)|^2$. Integrating $\rho(\boldsymbol{x},\alpha_0,t)$ thus obtained over $\alpha_0 = (\boldsymbol{x}_0,\boldsymbol{p}_0)$ with the weight $f(\boldsymbol{x}_0,\boldsymbol{p}_0)$, one gets the averaged density, denoted $n(\boldsymbol{x},t)$, namely, $n = \int \rho f d\alpha_0$. For the parameters used in the experiments and for ξ of the order of λ_T, at time $t = \tau_f$ when the interference pattern is measured, one has

$$\xi \ll \sqrt{\frac{\hbar\tau_f}{2m}}. \tag{32}$$

Making use of the relation in Eq. (32), one can compute the density (see Appendix A), obtaining

$$n(\boldsymbol{x},t) \simeq A_R^6 e^{-\frac{|\boldsymbol{x}|^2}{2R^2}}\left(1 + C_{\text{th}}\cos\frac{2\pi x}{\lambda_f}\right), \tag{33}$$

where

$$R = \sqrt{R_T^2 + \frac{k_B T \tau_f^2}{m} + \sigma^2} = \sqrt{R_T^2\left(1 + \omega^2\tau_f^2\right) + \sigma^2}. \tag{34}$$

The quantity R gives approximately the size of the expanded thermal cloud. Equation (33) predicts the contrast given in Eq. (22) for the interference pattern.

Finally, it would be of interest to say a few words on whether a notable improvement may be achieved for the agreement between C_{th} and C_{ex} at temperatures $T > T_d$, if the Boltzmann distribution is replaced by the Bose-Einstein distribution. We have performed numerical simulations but have not observed any obvious improvement (see Appendix B).

C. Predictions of the hybrid model

In this section, we discuss predictions of the hybrid model introduced in Sec. II B. In this model, the density of the cloud is written as

$$n(\boldsymbol{x}) = n_{\text{th}} + n_{\text{con}}, \tag{35}$$

where n_{con} indicates the contribution from the atoms in the coherently condensed state and n_{th} for that from the thermal atoms. The density n_{th} is in fact given by the right-hand side of Eq. (33) multiplied by $(1 - P_{\text{con}})$.

In the experiments, a contrast was obtained by measuring the intensity of the light reflecting from the atoms at the final stage [36]. It corresponds to the contrast given by

$n(x,y) = \int n(\boldsymbol{x})dz$. Since $R \gg \lambda_f$, the term $\exp(-\frac{|\boldsymbol{x}|^2}{2R^2})$ in Eq. (33) can be treated as 1 in the considered region. Then, for $n_{\rm th}(x,y) = \int n_{\rm th} dz$, we have

$$n_{\rm th}(x,y) \simeq (1 - P_{\rm con})A_R^4 \left(1 + C_{\rm th}\cos\frac{2\pi x}{\lambda_f}\right). \tag{36}$$

We use L to indicate the size of the region occupied by the atoms in the coherently condensed state. As discussed previously, the atoms in a coherently condensed state can be described by the same single-particle wave function when computing the interference pattern they generate. As long as the absolute value of this wave function changes slowly within region L, the density $n_{\rm con}(x,y) = \int n_{\rm con} dz$ has approximately the expression

$$n_{\rm con}(x,y) \approx \frac{P_{\rm con}}{L^2}\left(1 + \cos\frac{2\pi x}{\lambda_f}\right), \tag{37}$$

independent of the exact shape of the wave function [see Eq. (C7) in Appendix C].

Making use of Eqs. (35)–(37), after simple algebra, we get the following expression for the density of the atoms in the x-y plane,

$$n(x,y) \approx G\left(1 + C\cos\frac{2\pi x}{\lambda_f}\right), \tag{38}$$

where

$$G = (1 - P_{\rm con})A_R^4 + \frac{P_{\rm con}}{L^2}, \tag{39}$$

and the modified contrast is given by

$$C = \frac{(1 - P_{\rm con})C_{\rm th} + qP_{\rm con}}{(1 - P_{\rm con}) + qP_{\rm con}}, \tag{40}$$

with $q = 1/(L^2 A_R^4)$. Making use of the expression of A_R given by Eq. (3), one gets $q = \frac{2\pi R^2}{L^2}$. For the parameters used in the experiments, the main contribution to R in Eq. (34) is given by the term $\frac{k_B T \tau_f^2}{m}$; as a result,

$$\frac{q}{T} \approx \frac{2\pi k_B \tau_f^2}{mL^2}. \tag{41}$$

It is reasonable to assume that the size L of the coherently condensed state has a weak dependence on the temperature T. Then the ratio q/T is almost independent of T or changes slowly with T.

The expansion of the coherently condensed state should be much slower than that of the thermal cloud. This implies that the size L of the coherently condensed state should be much smaller than the size R of the thermal cloud. As a result, $q \gg 1$. Hence, even for small $P_{\rm con}$, it is possible for $qP_{\rm con}$ to be not small and to make a significant contribution to the predicted contrast C in Eq. (40). But for sufficiently small $P_{\rm con}$ for which $qP_{\rm con} \ll C_{\rm th}$, one has $C \simeq C_{\rm th}$; that is, the prediction of the hybrid model reduces to that of the simple thermal model.

D. Comparison with experimental results

In order to compare the above-obtained contrast in Eq. (40) and the experimental results, we consider a quantity M defined by

$$M = \frac{C - C_{\rm th}}{T^{3/2}(1 - C)}. \tag{42}$$

Substituting Eq. (18) with $\gamma = 2$ and $\beta = 0.5$ into Eq. (40), then into Eq. (42), and noting the smallness of $P_{\rm con}$, one gets

$$M \approx aE_{\frac{2}{3}}\left(\left(\frac{T}{T_0}\right)^{3/2}\right), \tag{43}$$

where

$$a = \frac{a_c q}{T} = \frac{a_0 a_2}{3}\frac{q}{T}. \tag{44}$$

Before giving the comparison, we discuss the properties of the two parameters T_0 and a in the studied experiments. First, let us consider T_0 in Eq. (20). As discussed in Sec. II C, the parameters a_1 and u_0 are almost temperature independent. The parameter a_2 given below Eq. (25) is also temperature independent. Hence, T_0 is temperature independent. The value of T_0 is in fact determined by intrinsic properties of the gas and by the initial condition (not including the temperature dependence) of the cloud in the trap. Hence, T_0 should also be independent of τ_p and λ_f. Next, for the parameter a in Eq. (44), as discussed in Sec. II C and Sec. III C, the parameter a_0 and the ratio q/T are almost temperature independent or change slowly with the temperature T. Hence, the parameter a is almost temperature independent or changes slowly with T.

An advantage of considering the quantity M as a function of the temperature T is that the parameter a introduces a vertical shift only to $\ln M$. Making use of this property and noting the above-discussed weak dependence of a on T, it is possible to approximately determine the value of T_0 by a best fitting of the prediction of Eq. (43) to the experimental results obtained with one pair of (τ_p, λ_f). With the value of T_0 thus obtained, one can check whether the prediction of Eq. (43) may be in agreement with the experimental results for this pair of (τ_p, λ_f) and, furthermore, also check for other pairs of (τ_p, λ_f).

We use the experimental data obtained with $\tau_p = 30\ \mu$s and $\lambda_f = 170\ \mu$m to get an estimate of the value of T_0. We found $T_0 = 5.12\ \mu$K ($a = 0.075\ \mu\text{K}^{-3/2}$) in the best fitting, given by the minimum of $s = \frac{1}{\sum_i 1}\sum_i (\ln M_{{\rm ex},i} - \ln M_i)^2$ ($s_{\rm min} = 0.012$), where $M_{{\rm ex},i}$ represents the values given by Eq. (42) from the experimentally obtained contrasts $C_{\rm ex}$ and M are the corresponding values given by Eq. (43). As shown in Fig. 2, in this best fitting, the agreement between $M_{\rm ex}$ and the theoretical predictions is good over almost the whole temperature range, except for the first two points with T close to T_d. Moreover, the agreement is also good in the contrast plot (Fig. 3).

Then we study the case of $\tau_p = 10\ \mu$s. We first fix T_0 at the above-obtained value of $T_0 = 5.12\ \mu$K and take a as a fitting parameter. More or less, agreement has been seen between the analytically predicted M in Eq. (43) and the experimental results in the temperature region $T \gtrsim T_d + 1\ \mu$K, where $C_{\rm ex}$ values are obviously larger than $C_{\rm th}$ values (see Fig. 4). Specifically, (i) for $\lambda_f = 230\ \mu$m with $T_d \approx 2\ \mu$K, the agreement is good in the temperature region $T \gtrsim 3\ \mu$K; and (ii) for $\lambda_f = 340\ \mu$m with $T_d \approx 3\ \mu$K, the agreement is not as good, but still not bad, in the region of $T \gtrsim 4\ \mu$K except for the last two points. Similar results can also be seen

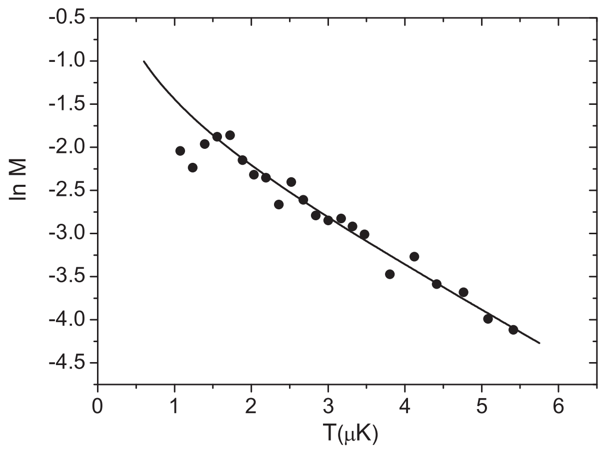

FIG. 2. The $\ln M$ versus the temperature T, for $\tau_p = 30\ \mu$s and $\lambda_f = 170\ \mu$m. Circles: experimental results computed from Eq. (42) with C replaced by the experimentally obtained contrasts $C_{\rm ex}$ given in Ref. [18]. Solid curve: analytical predictions computed from Eq. (43) with two fitting parameters, $a = 0.075\ \mu\mathrm{K}^{-1.5}$ and $T_0 = 5.12\ \mu$K.

in the contrast plot (Fig. 5). For $\lambda_f = 170\ \mu$m, no reasonable comparison can be made, because there are only one or two points in the region above $T_d + 1\ \mu$K.

Next, we take both T_0 and a as fitting parameters in the case of $\tau_p = 10\ \mu$s. (i) At $\lambda_f = 230\ \mu$m with 11 points satisfying $T > 3\ \mu$K, the best fitting gives $T_0 = 4.7\ \mu$K ($a = 0.053\ \mu\mathrm{K}^{-3/2}$ and $s_{\min} = 0.0109$), close to the value of 5.12 μK obtained in Fig. 2. (ii) At $\lambda_f = 340\ \mu$m, there exist eight points satisfying $T > 4\ \mu$K. With all eight points used, the best-fitting T_0 is much larger than 5.12 μK, while with the first six of the eight points used, the best fitting gives $T_0 = 3.45\ \mu$K ($a = 0.26\ \mu\mathrm{K}^{-3/2}$ and $s_{\min} = 0.0019$).

On the other hand, for a sufficiently small value of the parameter a such that $q P_{\rm con} \ll C_{\rm th}$, the contrasts predicted in the hybrid model in Eq. (40) are approximately equal to $C_{\rm th}$ and, hence, close to the experimental data $C_{\rm ex}$ in the region $T < T_d$ (see Fig. 5). (The value of T_0 does not influence the prediction for $a = 0$.) However, for whatever fixed value of the parameter a, the prediction of Eq. (40) for the contrast cannot be made to agree with the experimental data over the whole

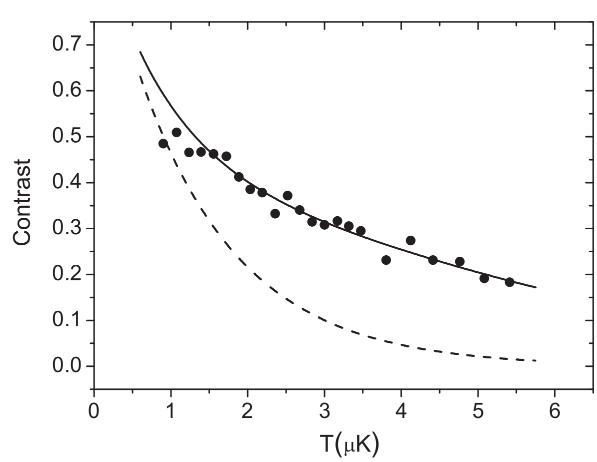

FIG. 3. Similar to Fig. 2, but for the contrast. The theoretical prediction (solid curve) was computed by making use of Eq. (42), with M computed from Eq. (43). For comparison, $C_{\rm th}$ values of the simple thermal model are also plotted (dashed curve).

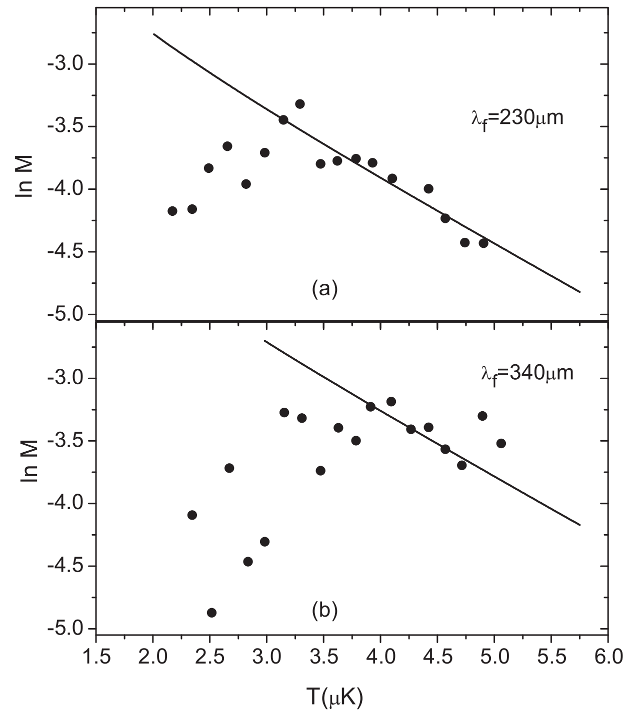

FIG. 4. Similar to Fig. 2, but for $\tau_p = 10\ \mu s$ with a fixed $T_0 = 5.12\ \mu K$. The fitting parameter $a = 0.044\ \mu\mathrm{K}^{-1.5}$ for $\lambda_f = 230\ \mu m$ and $a = 0.083\ \mu\mathrm{K}^{-1.5}$ for $\lambda_f = 340\ \mu$m.

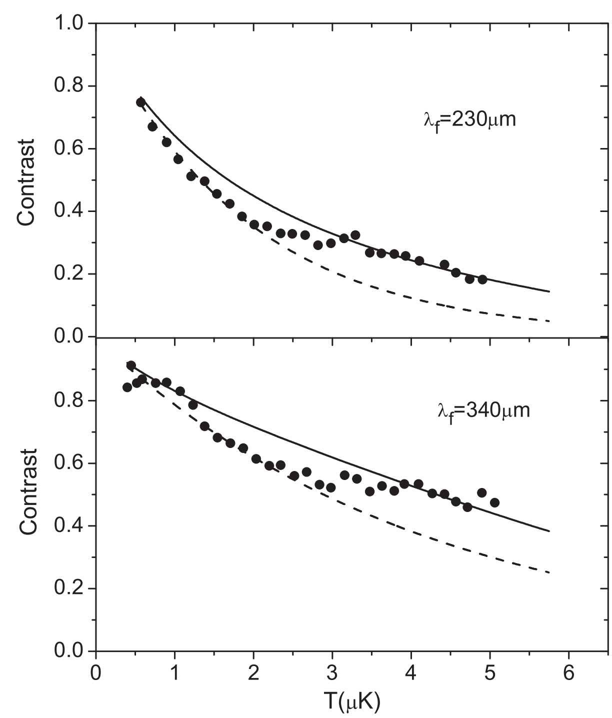

FIG. 5. Similar to Fig. 4, but for the contrast. The dashed curve represents $C_{\rm th}$.

temperature region. Even when we changed the value of T_0 as well, no obvious improvement was observed.

Therefore, in the case of $\tau_p = 10\ \mu$s, the contrast undergoes a transition approximately in the region $(T_d, T_d + 1\ \mu\text{K})$. Below this region the hybrid model works well with $a \approx 0$; above this region, the model works well at $\lambda_f = 230\ \mu$m with a as a fitting parameter and with T_0 fixed at the value determined in the above case of $\tau_p = 30\ \mu$s, and works partially at $\lambda_f = 340\ \mu$m. We note that this conclusion can also be regarded as being valid for $\lambda_f = 170\ \mu$m.

To summarize, in the case of $\tau_p = 30\ \mu$s, the hybrid model can explain the main features of the experimental results of the contrasts over almost the whole temperature region studied experimentally. However, in the case of $\tau_p = 10\ \mu$s, in order to explain the main features of the experimental results by the hybrid model, one needs to assume that the contrast undergoes a transition approximately in the region $(T_d, T_d + 1\ \mu\text{K})$, below which the parameter $a \approx 0$ and above which a has a nonzero value.

A hint to the possible origin of the above-discussed transition behavior of the contrast lies in an observation made in Ref. [18]. That is, in the case of $\tau_p = 30\mu$s the two Bragg beams have a significant velocity-selection effect, meanwhile, in the case of $\tau_p = 10\ \mu$s the velocity-selection effect is not as significant. This suggests that the velocity-selection effect of the Bragg beams may have some relation to the transition behavior of the contrast.

IV. DISCUSSION AND CONCLUDING REMARKS

In this paper, we study the conjecture that, in a gas at a temperature above, but not much above, the BEC transition temperature, a small portion of the atoms may lie in a coherently condensed state. We show that experimental support for this conjecture exists; that is, with a hybrid model based on this conjecture, some unexplained experimental results reported in Ref. [18] can be explained.

What is left unexplained is the transition behavior of the contrast, from a relatively low-temperature region, in which the atoms behave like thermal atoms, to a relatively high-temperature region, in which some of the atoms show quantum coherence like that in a coherently condensed state. In order to understand this transition behavior, further investigations, both experimental and theoretical, are needed. A key point may lie in the role played by a velocity-selection feature of the Bragg beams. In particular, one may wonder whether any relation exists between the velocity-selection effect and the formation of a coherently condensed or some BEC-type state among some atoms. To solve this problem is a challenging task. In fact, the mechanism of the formation of BEC is a topic that is not fully understood, though many efforts have been made and important progress has been achieved [8–16,37–39]. From the experimental viewpoint, e.g., it should be useful to study the possible connection between the transition region discussed above and the velocity-selection effect of the Bragg beams, in particular, in the case of $\tau_p = 10\ \mu$s. Moreover, a study of the contrasts at temperatures higher than those reported in Ref. [18] should be of interest too.

Finally, we give a brief discussion of experiments that may be performed in the future to test other aspects of the hybrid model proposed in this paper. The theory discussed here predicts that the value of T_0 [Eq. (20)] is a function of the parameter a_1 in the decoherence rate [see Eq. (14)]. Decreasing the scattering length by the technology of Feshbach resonance [5], the parameter a_1 should be decreased, and as a result, the value of T_0 should increase. This implies an increase in the proportion of the condensed part (P_{con}), hence, an increase in the contrast, which may be tested by experiments. When the scattering length is decreased to a sufficiently small value, it is possible for T_0 to be sufficiently large such that P_{con} does not show an obvious decay in the temperature region studied. In this case, since $q \propto T$, Eq. (40) shows that it may even be possible for the contrast to increase with increasing temperature.

ACKNOWLEDGMENTS

W.W. is grateful to Jie Liu for initial stimulating discussions and is also grateful to Jiangbin Gong for valuable suggestions. This work was partially supported by the Natural Science Foundation of China under Grants No. 11275179 and No. 10975123 and the National Key Basic Research Program of China under Grant No. 2013CB921800.

APPENDIX A: DERIVATION OF EQ. (33)

In order to derive Eq. (33), let us first compute the phase difference between $\psi_1(t)$ and $\psi_2(t)$ in Eq. (31). At time $t = \tau_f$, Eqs. (30) and (32) give $\sigma \approx \frac{\hbar t}{2m\xi}$. Then, making use of expression (29), it is easy to get the expression of the phase difference,

$$-\frac{\boldsymbol{p}_0 \cdot \boldsymbol{d}}{\hbar} + \frac{\left[\boldsymbol{x} - \left(\boldsymbol{x}_t + \frac{\boldsymbol{d}}{2}\right)\right]^2 - \left[\boldsymbol{x} - \left(\boldsymbol{x}_t - \frac{\boldsymbol{d}}{2}\right)\right]^2}{4\sigma\xi}, \tag{A1}$$

where

$$\boldsymbol{x}_t = \boldsymbol{x}_0 + \frac{\boldsymbol{p}_0 t}{m}. \tag{A2}$$

Simple algebra shows that the difference has the simple expression

$$\frac{2\pi(x - x_0)}{\lambda_f}, \tag{A3}$$

where λ_f is defined in Eq. (23). Then the density is written as

$$\begin{aligned} \rho(\boldsymbol{x},\alpha,t) &= |\psi(\boldsymbol{x},\alpha,t)|^2 \\ &\approx \frac{1}{2} A_\sigma^6 e^{-\frac{(\boldsymbol{x}-\boldsymbol{x}_t)^2}{2\sigma^2}} \\ &\quad \times \left[e^{\frac{(x-x_t)d}{2\sigma^2}} + e^{-\frac{(x-x_t)d}{2\sigma^2}} + 2\cos\frac{2\pi(x - x_0)}{\lambda_f} \right]. \end{aligned} \tag{A4}$$

Integrating Eq. (A4) with the weight f in Eq. (24) over $\alpha = (\boldsymbol{x}_0, \boldsymbol{p}_0)$, one gets Eq. (33).

APPENDIX B: CONTRAST IN THE SIMPLE THERMAL MODEL WITH A BOSE-EINSTEIN DISTRIBUTION

In this Appendix, by numerical simulation, we show that, in the simple thermal model with a Bose-Einstein distribution

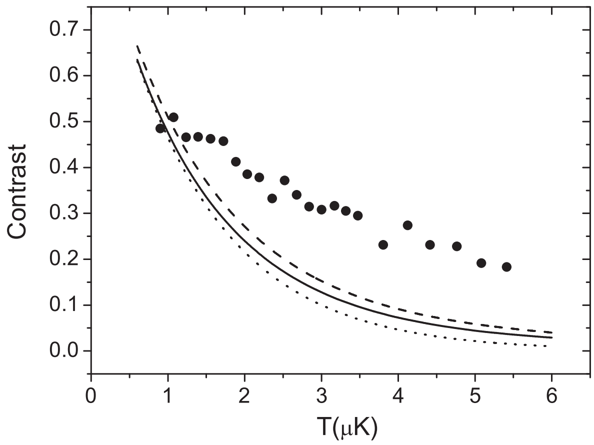

FIG. 6. Contrasts predicted by Eq. (B2), in the simple thermal model with the Bose-Einstein distribution. Dash curve: $\mu = 0$. Solid curve: $\mu = -1\ \mu$K. For comparison, predictions of Eq. (22) with the Boltzmann distribution (dotted curve) and experimental data with $\lambda_f = 170\ \mu$m, $\tau_p = 30\ \mu$s (filled circles) are also plotted.

for the function f in Eq. (24), the obtained contrasts are still not close to the experimental results in the temperature region $T > T_d$. The Bose-Einstein distribution is written as

$$f_{\text{BE}}(\boldsymbol{x_0},\boldsymbol{p_0}) = \frac{1}{e^{(E-\mu)/k_BT} - 1}, \tag{B1}$$

where $E = \frac{\boldsymbol{p_0}^2}{2m} + \frac{m\omega^2\boldsymbol{x_0}^2}{2}$ is the single-particle energy in the trap and μ is the chemical potential. Under this distribution, direct computation shows that, in the simple thermal model, the contrast has the expression

$$\widetilde{C}_{\text{th}} = \frac{1}{\sum_{n=1}^{\infty}\frac{1}{n^3}z^n}\left\{\sum_{n=1}^{\infty}\frac{1}{n^3}z^n\exp\left(-\frac{2\pi^2R_T^2}{n\lambda_f^2}\right)\right\}, \tag{B2}$$

where $z = e^{\mu/k_BT}$. Taking the first-order terms in both the numerator and the denominator, Eq. (B2) gives C_{th} in Eq. (22). For a Bose gas, $\mu < 0$, hence $z < 1$. Numerically, we found that predictions of Eq. (B2) are not close to the experimental data for $T > T_d$, as illustrated in Fig. 6.

APPENDIX C: CONTRAST FOR A CLASS OF THE INITIAL CONDITIONS

In this Appendix, we discuss the contrast under initial conditions of a type more generic than Gaussian wave packets. It is shown that the expression of the contrast C_{th} in Eq. (22), as well as the expression of the fringe spacing λ_f in Eq. (23), is still approximately valid for a more generic type of single-particle states in the simple thermal model.

For simplicity, we discuss a one-dimensional configuration space. We consider an initial packet $\varphi_0(x)$, centered at x_0 in the coordinate space and at p_0 in the momentum space. We assume that the main body of the packet lies in a region of scale l, namely, $|x - x_0| \leqslant l$, not necessarily of a Gaussian shape. Free expansion of the packet gives

$$\varphi(x,t) = \frac{1}{2\pi\hbar}\int dp\,dx'\exp\left[-\frac{ip^2t}{2m\hbar} + \frac{ip(x-x')}{\hbar}\right]\varphi_0(x'). \tag{C1}$$

Changing the variable p to $p' = p - \frac{m(x-x')}{t}$, then integrating out p', we get

$$\varphi(x,t) = \sqrt{\frac{m}{2i\pi\hbar t}}\int dx'\exp\left(\frac{i(x-x')^2m}{2\hbar t}\right)\varphi_0(x'). \tag{C2}$$

Let us write the wave function beyond the two Bragg beams as

$$\psi_0(x) = \varphi_0(x) + \varphi_0(x+d). \tag{C3}$$

Making use of Eq. (C2), simple derivation gives the following expression for the time evolution of ψ:

$$\psi(x,t) = \sqrt{\frac{m}{2i\pi\hbar t}}\int dx'\exp\left(\frac{i(x-x')^2m}{2\hbar t}\right)\varphi_0(x') \times\left[1 + \exp\left(\frac{id(2x-2x'+d)m}{2\hbar t}\right)\right]. \tag{C4}$$

For times sufficiently long, one has $l \ll \lambda$, where

$$\lambda = \frac{ht}{md}. \tag{C5}$$

Since the main body of $\varphi_0(x')$ lies within a region of scale l centered at x_0, in the integration on the right-hand side of Eq. (C4), approximately, one may consider the integration domain $(x_0 - l, x_0 + l)$. Within this region, because of the relation $l \ll \lambda$, the variable x' in the term $\exp(\frac{id(2x-2x'+d)m}{2\hbar t})$ can be approximately taken as x_0. Then, making use of Eq. (C2), Eq. (C4) can be written as

$$\psi(x,t) \approx \varphi(x,t)\left[1 + \exp\left(i\frac{2\pi\left(x - x_0 + \frac{d}{2}\right)}{\lambda}\right)\right]. \tag{C6}$$

This gives

$$\rho(x,t) \approx |\varphi(x,t)|^2\left(1 + \cos\frac{2\pi\left(x - x_0 + \frac{d}{2}\right)}{\lambda}\right). \tag{C7}$$

For a slowly varying $|\varphi(x,t)|^2$, Eq. (C7) predicts an interference pattern with a fringe spacing λ under an envelope $|\varphi(x,t)|^2$. Note that λ gives λ_f in Eq. (23) at $t = \tau_f$.

For an ensemble of packets, with x_0 and p_0 obeying the Boltzmann distribution [cf. Eq. (24)], direct derivation gives the expression for the density,

$$n(x) \approx F_0(x) + F_1(x)\cos\frac{2\pi\left(x + \frac{d}{2}\right)}{\lambda} + F_2(x)\sin\frac{2\pi\left(x + \frac{d}{2}\right)}{\lambda}, \tag{C8}$$

where

$$F_0(x) = \int dx_0 G(x,x_0)\exp\left(-\frac{x_0^2}{2R_T^2}\right),$$
$$F_1(x) = \int dx_0 G(x,x_0)\exp\left(-\frac{x_0^2}{2R_T^2}\right)\cos\frac{2\pi x_0}{\lambda}, \tag{C9}$$
$$F_2(x) = \int dx_0 G(x,x_0)\exp\left(-\frac{x_0^2}{2R_T^2}\right)\sin\frac{2\pi x_0}{\lambda}.$$

Here,

$$G(x,x_0) = \frac{\hbar\omega}{k_B T}\int \mathrm{d}p_0 |\varphi(x,t;x_0,p_0)|^2 \exp\left(-\frac{p_0^2}{2mk_BT}\right), \tag{C10}$$

with the dependence on x_0 and p_0 written explicitly.

In some situations of interest, the quantity $G(x,x_0)$ can be approximately regarded as a constant for x in the region of measurement, i.e., for x of the order of λ and for x_0 in a region wherein $\exp(-\frac{x_0^2}{2R_T^2})$ is not small. To be specific, we discuss two examples. In the first example, $|\varphi|^2 \propto \delta(x - x_0 - p_0 t/m)$. This gives

$$G(x,x_0) \propto \exp\left[-\frac{(x-x_0)^2}{2L_t^2}\right], \tag{C11}$$

where $L_t = \sqrt{k_B T t^2/m}$. For the parameters used in the experiments in Ref. [18], direct computation shows that $\lambda/L_t = (\sqrt{2\pi}\lambda_T)/d$ is approximately between $1/3$ and $1/15$, and $R_T/L_t = 1/\omega t \approx 1/20$ for $t = \tau_f$. Hence, G is approximately a constant for the value of x and x_0 of interest here. In the second example, $|\varphi|^2$ has a Gaussian form with a standard deviation σ, i.e., $|\varphi|^2 \propto \exp[-(x - x_0 - p_0 t/m)^2/(2\sigma^2)]$, like that in the thermal model discussed above. In this case,

$$G(x,x_0) \propto \exp\left[-\frac{(x-x_0)^2}{2(L_t^2+\sigma^2)}\right]. \tag{C12}$$

Similarly, G is approximately a constant in the region of interest here.

For an approximately constant G, $F_2 \approx 0$ and can be neglected. Then direct computation shows that

$$n(x) \approx F_0\left[1 + C_{\mathrm{th}}\cos\frac{2\pi\left(x+\frac{d}{2}\right)}{\lambda}\right], \tag{C13}$$

where C_{th} is the contrast given in the simple thermal model in Eq. (22).

[1] M. H. Anderson, J. R. Ensher, M. R. Matthews, C. E. Wieman, and E. A. Cornell, Science **269**, 198 (1995).
[2] K. B. Davis, M.-O. Mewes, M. R. Andrews, N. J. van Druten, D. S. Durfee, D. M. Kurn, and W. Ketterle, Phys. Rev. Lett. **75**, 3969 (1995).
[3] C. C. Bradley, C. A. Sackett, and J. J. Tollett, and R. G. Hulet, Phys. Rev. Lett. **75**, 1687 (1995).
[4] K. Huang, *Statistical Mechanics*, 2nd ed. (John Wiley and Sons, New York, 1987).
[5] C. J. Pethick and H. Smith, *Bose-Einstein Condensation in Dilute Gases* (Cambridge University Press, Cambridge, 2002).
[6] A. J. Leggett, Rev. Mod. Phys. **73**, 307 (2001).
[7] F. Dalfovo, S. Giorgini, L. P. Pitaevskii, and S. Stringari, Rev. Mod. Phys. **71**, 463 (1999).
[8] P. B. Blakie, A. S. Bradley, M. J. Davis, R. J. Ballagh, and C. W. Gardiner, Adv. Phys. **57**, 363 (2008).
[9] H. T. C. Stoof, J. Low Temp. Phys. **114**, 11 (1999).
[10] H. T. C. Stoof and M. J. Bijlsma, J. Low Temp. Phys. **124**, 431 (2001).
[11] C. W. Gardiner and M. J. Davis, J. Phys. B: At. Mol. Opt. Phys **36**, 4731 (2003).
[12] N. G. Berloff and B. V. Svistunov, Phys. Rev. A **66**, 013603 (2002).
[13] P. B. Blakie and M. J. Davis, Phys. Rev. A **72**, 063608 (2005).
[14] E. Calzetta, B. L. Hu, and E. Verdaguer, Int. J. Mod. Phys. B **21**, 4239 (2007).
[15] A. Bezett, E. Toth, and P. B. Blakie, Phys. Rev. A **77**, 023602 (2008).
[16] C. W. Gardiner and P. Zoller, Phys. Rev. A **55**, 2902 (1997); **58**, 536 (1998); **61**, 033601 (2000); D. Jaksch, C. W. Gardiner, and P. Zoller, *ibid.* **56**, 575 (1997); D. Jaksch, C. W. Gardiner, K. M. Gheri, and P. Zoller, *ibid.* **58**, 1450 (1998); M. D. Lee and C. W. Gardiner, *ibid.* **62**, 033606 (2000); M. J. Davis, C. W. Gardiner, and R. J. Ballagh, *ibid.* **62**, 063608 (2000).
[17] L. You, W. Hoston, and M. Lewenstein, Phys. Rev. A **55**, R1581 (1997); L. You and M. Holland, *ibid.* **53**, R1 (1996).
[18] D. E. Miller, J. R. Anglin, J. R. Abo-Shaeer, K. Xu, J. K. Chin, and W. Ketterle, Phys. Rev. A **71**, 043615 (2005).
[19] A. O. Caldeira and A. J. Leggett, Physica A **121**, 587 (1983).
[20] B. L. Hu, J. P. Paz, and Y. Zhang, Phys. Rev. D **45**, 2843 (1992).
[21] J. J. Halliwell and T. Yu, Phys. Rev. D **53**, 2012 (1996).
[22] G. W. Ford and R. F. O'Connell, Phys. Rev. D **64**, 105020 (2001).
[23] J. Eisert, Phys. Rev. Lett **92**, 210401 (2004).
[24] K. Hornberger, Phys. Rev. Lett **97**, 060601 (2006).
[25] U. Weiss, *Quantum Dissipative Systems* (World Scientific, Singapore, 1999).
[26] H. D. Zeh, Found. Phys. **1**, 69 (1970); **3**, 109 (1973).
[27] E. Joos, H. D. Zeh, C. Kiefer, D. Giulini, J. Kupsch, and I.-O. Stamatescu, *Decoherence and the Appearance of a Classical World in Quantum Theory*, 2nd ed. (Springer, Berlin, 2003).
[28] W. H. Zurek, Phys. Rev. D **24**, 1516 (1981); **26**, 1862 (1982).
[29] W. H. Zurek, Rev. Mod. Phys. **75**, 715 (2003).
[30] M. Schlosshauer, Rev. Mod. Phys. **76**, 1267 (2004).
[31] W.-G. Wang, L. He, and J. Gong, Phys. Rev. Lett. **108**, 070403 (2012).
[32] A. Perelomov, *Generalized Coherent State and Their Applications* (Springer-Verlag, Berlin, 1986)
[33] D. A. R. Dalvit, J. Dziarmaga, and W. H. Zurek, Phys. Rev. A **72**, 062101 (2005).
[34] At temperatures T much higher than T_c, the density of atoms with $\xi > d_a$ may become so low that a considerable proportion of these atoms are not in a mutual-coherence relationship. In this case, one may introduce a parameter c_1 before the integration on the right-hand side of Eq. (9), with c_1 obviously less than 1.
[35] See, e.g., C. Cohen-Tannoudji, B. Diu, and F. Laloë, *Quantum Mechanics*, Vol. 1 (Wiley, Paris, 1977), p. 64.
[36] W. Ketterle (private communication).
[37] Yu. Kagan, E. L. Surkov, and G. V. Shlyapnikov, Phys. Rev. A **54**, R1753 (1996).
[38] Yu. Kagan and B. V. Svistunov, Phys. Rev. Lett. **79**, 3331 (1997).
[39] Y. Castin and R. Dum, Phys. Rev. A **57**, 3008 (1998).